Muhammad Riaz, Muhammad Ajmal*, Atif Naseem, Nusrat Jabeen, Zahoor H. Farooqi, Khalid Mahmood, Abid Ali, Lubna Rasheed and Ahmad Nauman Shah Saqib

Synthesis of poly (N-isopropyl acrylamide-co-2-acrylamido methylpropane sulfonic acid) hydrogel containing copper and nickel nanoparticles with easy recycling and efficient catalytic potential

https://doi.org/10.1515/zpch-2022-0107
Received July 21, 2022; accepted October 20, 2022; published online November 1, 2022

Abstract: Poly(N-isopropyl acrylamide-co-2-acrylamido methyl propane sulfonic acid) hydrogel was prepared and used as matrix for the fabrication of nickel and copper nanoparticles. Nickel and copper nanoparticles were fabricated via *in situ* reduction of Ni (II) and Cu (II) ions within the hydrogel matrix. The manufactured hydrogel and its corresponding composites with Ni and Cu nanoparticles were characterized by FTIR, XRD, EDX, TEM, and TGA. Thermal stability of hydrogel was found to be increased upon fabricating with metal nanoparticles. The hydrogel showed ability to absorb water 63 times of its weight in dried form. The Ni and Cu nanoparticles were observed to be well dispersed, spherical in shape and most of them were having diameters in the range of 12.5 to 38.8 nm and 58 to 102 nm, respectively. The as-prepared hydrogel-nickel and hydrogel-Cu nanocomposite were used as catalysts for the reduction of a toxic pollutant 4-nitrophenol. At 25 °C, the reduction of 4-NP was found to proceed with apparent rate constant (k_{app}) of 0.107 and 0.122 min^{-1} in the presence of composite containing Ni and Cu nanoparticles, respectively. However, k_{app} was increased with corresponding increase in

***Corresponding author: Muhammad Ajmal**, Department of Chemistry, Division of Science and Technology, University of Education, Lahore, Pakistan, E-mail: m.ajmal65@yahoo.com
Muhammad Riaz and Nusrat Jabeen, Department of Chemistry, University of Wah, Wah Cantt, Pakistan
Atif Naseem, Lubna Rasheed and Ahmad Nauman Shah Saqib, Department of Chemistry, Division of Science and Technology, University of Education, Lahore, Pakistan
Zahoor H. Farooqi, School of Chemistry, University of the Punjab, New Campus, Lahore, Pakistan
Khalid Mahmood, Institute of Chemical Sciences, Bahauddin Zakariya University, Multan, Pakistan
Abid Ali, Department of Chemistry, University of Lahore, Lahore, Pakistan

temperature and its maximum value was found to be 0.815 min^{-1} at 88 °C with catalyst containing Ni nanoparticles. The formation of well dispersed Ni and Cu nanoparticles in the prepared hydrogel reflected that this hydrogel system can act as efficient stabilizing agent along with acting as a reactor medium. Recycling potential of catalysts was studied for five successive cycles.

Keywords: catalysts; copper nanoparticles; hydrogel; nickel nanoparticles.

1 Introduction

Water is potentially a valuable resource because its availability is vital for the survival of all living creatures on our planet. With the rapid development in technologies and industries in the last few decades, organic waste contamination in water has been continuously increased and becoming crucial issue with every passing day [1]. According to UN assessment report, pure and freshwater supply is a worldwide issue that has become a challenge for the entire planet in the twenty-first century since the survival of living organisms is endangered by contaminated water. Among various water contaminants, 4-nitrophenol (4-NP) is of great concern because of its wide use. 4-NP persists in water for a long period and its biological breakdown is very difficult. 4-NP is ecologically harmful substance having highly toxic and carcinogenic effect on humans [2, 3]. Scientists are seeking for ways to remove 4-NP from aquatic systems or convert it to less hazardous compound. Adsorption, catalysis, chemical oxidation and reduction, biological treatment, and photocatalytic degradation are some of the chemical and physical approaches that had been employed to treat water containing 4-NP [4–7]. Catalytic degradation or conversion of water contaminants to less toxic and useful compounds have become the most suitable of the above-mentioned techniques because it is energy-efficient, affordable, ecofriendly, and remarkable efficiency for the elimination/reduction of contaminates. 4-NP can also be reduced to a less toxic and further useful compound 4-aminophenol (4-AP) by using a mild reducing agent and suitable catalyst [8, 9]. 4-AP is used in pharmaceutical fields for the synthesis of many antipyretic and analgesic drugs like paracetamol, phenacetin, and acetanilide [10, 11]. Therefore, conversion of 4-NP to 4-AP is a valuable way to get rid of toxicity of 4-NP. In this approach, we cannot only get rid of a toxic material but also obtain a useful compound from that toxin. The metal nanoparticles (NPs) have become fascinated catalysts for the reduction of 4-NP in the last few decades due to their higher surface to volume ratio and surface energy. NPs have shown efficient catalytic potential for a variety of processes. For example, dehydrogenation of alcohol can be catalyzed with silver NPs [12], electro-oxidation of formic acid can be catalyzed

with platinum NPs [13], and oxidation of carbon monoxide (CO) can be catalyzed with platinum-gold NPs [14]. The catalytic activity of metal NPs varies with the presence of active sites on their surface. When the surface area increases the number of active sites on the surface increases which in turn enhances the catalytic activity. As the specific surface area and surface energy of tiny nanoparticles are higher, they aggregate if not stabilized by suitable stabilizing agent. The aggregation causes a decrease in the active sites which in turn leads to a significant loss in catalytic activity. This issue greatly limits the implementation of valuable metallic nanoparticles as catalysts in practical processing [15]. To address this problem, catalytic nanoparticles are often stabilized by polymers or other suitable solid supports, which also permit catalyst recycling. Some supporting materials are dendrimers, silica, alumina, microfiber, collides and hydrogels [16–24].

Among various supporting materials hydrogels got more fascination because of their hydrophilic character, flexibility/pliability and three-dimensional (3-D) pattern of structure [25]. Furthermore, hydrogel materials are more beneficial because of their chemical and physical stability, recyclability, affordable price and non-toxic nature [25, 26]. Swelling behavior of hydrogel materials make them prominent from other materials. The swelling behavior of hydrogels is supported by their pliable polymeric network, enabling them to retain sufficient volume of water without disintegrating [27]. Cleansing of polluted water [28, 29], tissue engineering [30], targeted medicine delivery [31], improved oil recovery [32, 33], bio-nanotechnology [34, 35], production and stabilization of inorganic nanoparticles [36–38], and biomedical implants [39, 40] have all sparked interests in these hydrophilic material. Hydrogels can be used as reactor mediums for the controlled synthesis of metal nanoparticles. Hydrogels contain metal-binding active sites such as –COOH, —SH, –OH, $-SO_3H$, and $-NH_2$ depending on their composition, which enable them to load significant quantities of metallic ions. The loaded metallic ions are securely attached in the hydrogel network due to electrostatic attractions of the metal binding sites and can be transformed into nanoparticles via chemical reduction. Hydrogels are also helpful in preparing NPs with controlled morphology within their 3-D network by changing the cross-linking density or chemical composition. The 3-D networks of hydrogels and functional groups present in those networks stabilize the metal nanoparticles and prevent their aggregation. The as-prepared hydrogel-metal NPs composite can be applied as catalyst. The porous structure and chemical functional groups support the diffusion of reactants towards/into the hydrogel network to get adsorbed on the surface of NPs to react with each other. Moreover, easy separation of hydrogel-metal NPs composite from the rection mixture via filtration makes them reusable for many times. Precious noble metal nanoparticles such as gold (Au), pallidum (Pd), and platinum (Pt) have been explored as catalysts for the reduction of 4-NP to 4-AP [24, 41–46]. Despite of the excellent catalytic potential, these noble metal NPs could not be considered for

application at large industrial scale due to their high price. Alternatively, nanoparticles of transition metals are being explored as catalyst. In this regard, we synthesized Ni and Cu nanoparticles using poly(N-Isopropyl acrylamide-co-2-acrylamido methyl propane sulfonic acid) hydrogel (HG) as a stabilizer and explored their catalytic capability in the reduction of 4-NP.

2 Materials

N-isopropylacrylamide (NIPAM, 97%) and 2-acrylamido-2-methylpropane sulfonic acid (AMPS, 99%) were purchased from Merck. Ammonium persulphate (APS, 97%), N,N-methylenebisacrylamide (NNMBA, 99%) and N,N,N,N-tetramethylethylenediamine (TEMED, 100%) were purchased from Riedel-Dehaan, Panreac, and VWR, respectively. Chemicals were utilized as procured. Nickel chloride hexahydrate ($NiCl_2$, 98%) and copper chloride ($CuCl_2$, 97%) were purchased from Merck and Sigma Aldrich, respectively. Deionized water was used wherever it was required in this study.

2.1 Preparation of HG

The bulk HG was prepared at room temperature. The transparent solutions of NIPAM (0.0044 mol in 3 mL deionized water), AMPS (0.0044 mol in 1 mL deionized water) were first prepared in separate glass vials and then mixed with each other in a single glass vial. The mixture was added with 0.088 mmol of each of the MBA and APS and homogenized again. As a last reagent, 200 µL of TEMED was added in the reaction mixture with the help of a micropipette. The reaction mixture was homogenized again by high-speed stirring and then transferred to plastic straws. The reaction mixture was allowed to react without any disturbance for 24 h. The prepared semisolid hydrogel was taken out from the straws and sliced into small pieces. The hydrogel was washed by plunging it in deionized water for 4 days to remove the impurities. The deionized water was changed twice a day after regular intervals. Finally washed hydrogel pieces were shifted to polystyrene plates which were placed in oven at 70 °C for drying till constant weight. The obtained hydrogel was hard and uncompressible. Dried hydrogel was preserved in a glass vial with sample code.

2.2 Fabrication of metal nanoparticles in hydrogel

The fabrication of Ni and Cu nanoparticles in the prepared bulk HG was carried out in two steps. In the first step, the Ni (II) and Cu (II) ions were first loaded in the hydrogel by adding its 0.1 g separately in 1000 ppm aqueous solution of Ni (II) and Cu (II) ions, respectively. Overnight stirring was done to load the maximum amount of metal ions in the hydrogel. Filtered out the metal ions loaded hydrogel and subsequently washed with distilled water. These metal ions loaded hydrogel samples were transferred to polystyrene plates and dried at 70 °C till constant weight. In the second step, a 0.02 g of dried Ni (II) or Cu (II) ions loaded hydrogel was weighed and treated with 0.12 g of sodium borohydride in 30 mL distilled water in a beaker for 30 min. Finally, metal nanoparticles loaded hydrogel was filtered out through plankton cloth filter, followed by washing with water and its addition in the reaction mixture as catalyst or drying of hydrogel at 80 °C till constant weight for characterization.

2.3 Catalytic reaction

The catalytic test of the freshly prepared hydrogel-metal nanocomposite was conducted by using it in the reduction of 4-nitrophenol. The reaction was supervised/examined by UV-Vis spectrophotometer. The reaction was conducted in a temperature-controlled oil bath. The temperature of the oil bath was adjusted at least 2 h before starting the reaction. A 1000 mL, 0.001 M aqueous solution of 4-nitrophenol was prepared in volumetric flask and its 50 mL was used in a typical reaction. A 0.189 g of sodium borohydride and 0.03 g of freshly prepared hydrogel-metal nanocomposite was added into the 50 mL, 0.001 M aqueous solution of 4-nitrophenol as reducing agent and catalyst, respectively. The reaction was carried out at a desired temperature i.e., 25, 48, 56, or 88 °C and kept constant till the end of the reaction.

After specific time intervals, 0.5 mL of reaction mixture was withdrawn with micropipette and transferred into a test tube, already containing 7.5 mL of deionized water dilution. The absorption spectrum of the diluted sample was recorded in the wavelength range of 300–700 nm with UV-Visible spectrophotometer. The reaction was allowed to continue in reaction flasks at the set temperature and its monitoring was continued till minimum absorbance was recorded at 400 nm. For recycling, the catalyst was separated out from the reaction mixture by filtration and washed with deionized water. The recycled catalyst was used again for another cycle of the same reaction of 4-nitrophenol reduction under the same conditions.

3 Results and discussion

3.1 Synthesis and morphology of HG fabricated with nanoparticles

HG was prepared through free radical polymerization. In this polymerization process, once the free radicals are generated, the monomers and cross-linking agent react simultaneously to produce hydrogel network. The prepared hydrogel was used as stabilizer for the fabrication of Ni and Cu nanoparticles. The fabrication of nanoparticles was carried out by absorption of these metal ions form their aqueous solution into the hydrogel network followed by their reduction with sodium borohydride. The tendency of amide and sulfonic acid groups to attract the metal ions acts as deriving force for the absorption of Ni and Cu ions. The absorption of Ni and Cu ions was physically observed by the impartation of green and blue color, respectively, as shown in Figure 1 by image (a) and (b).

After treating with excess amount of reducing agent, the color of metal ions loaded hydrogel was converted into black as shown by image (c) which indicated the formation of metal nanoparticles in hydrogel network. The monomers and hydrogel were subjected to FTIR spectroscopic analysis to identify the polymerization and chemical composition of the hydrogel. Figure 2(a) and (b) represents the FTIR spectra of AMPS and NIPAM, respectively, while Figure 3(a–c) represents the FTIR

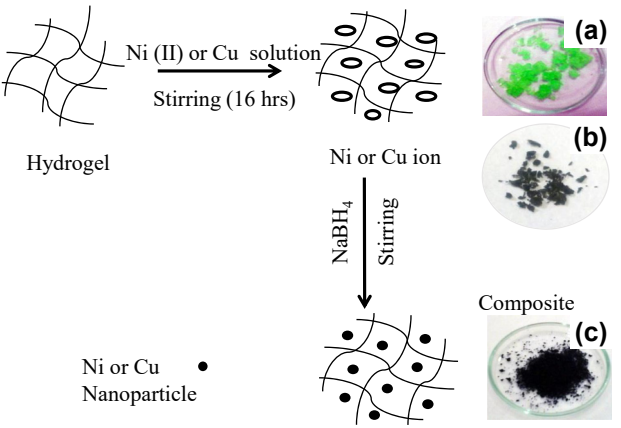

Figure 1: Schematic representation for the synthesis of Ni and Cu nanoparticles containing HG and digital camera images of HG loaded with (a) Ni (II) ions and (b) Cu (II) ions and (c) Ni or Cu nanoparticles.

spectra of bare hydrogel, Ni nanoparticles containing hydrogel and Cu nanoparticles containing hydrogel, respectively.

The monomers (NIPAM and AMPS) contain C=C absorption band at 1619 cm^{-1} and 1612 cm^{-1} respectively, while after complete polymerization C=C absorption band was disappeared in the spectra of HG. Also, C=C absorption band was not observed in hydrogel containing Ni and Cu nanoparticles. To support the presence of cross-linker in the bare hydrogel there are adsorption peaks at 1647 cm^{-1} and 1531 cm^{-1} correspond to-N-H scissoring and bending of amide group, respectively. The broad absorption band in the region of 3100 cm^{-1} to 3500 cm^{-1} corresponds to the overlapping of absorption bands of N-H and O-H. In case of hydrogel, the appearance of broad band of-OH indicates hydrogen bonding due to imbibed molecules of water in the network of hydrogel and approves the hydrophilic nature of HG. The absorption band value of S=O (asym.) at 1175 cm^{-1} indicates the existence of sulphonate groups of AMPS monomer in the hydrogel making it hydrophobic in nature. The peak shifting of S=O (asym.) at 1182 cm^{-1} indicates the presence of sulphonate groups of AMPS monomer in both Ni and Cu nanoparticles composite hydrogel. The shift in the absorption bands associated to NHC=O, N-H (bending) and C-N (stretching) in the metal nanoparticle containing hydrogel can be observed to the interaction of these functional groups with metals NPs and hence indicates the fabrication of metal nanoparticles in the HG.

The amide and sulfonic acid groups in the HG are hydrophilic in nature and make it capable to absorb water. In the absence of water, the polymer chains in the

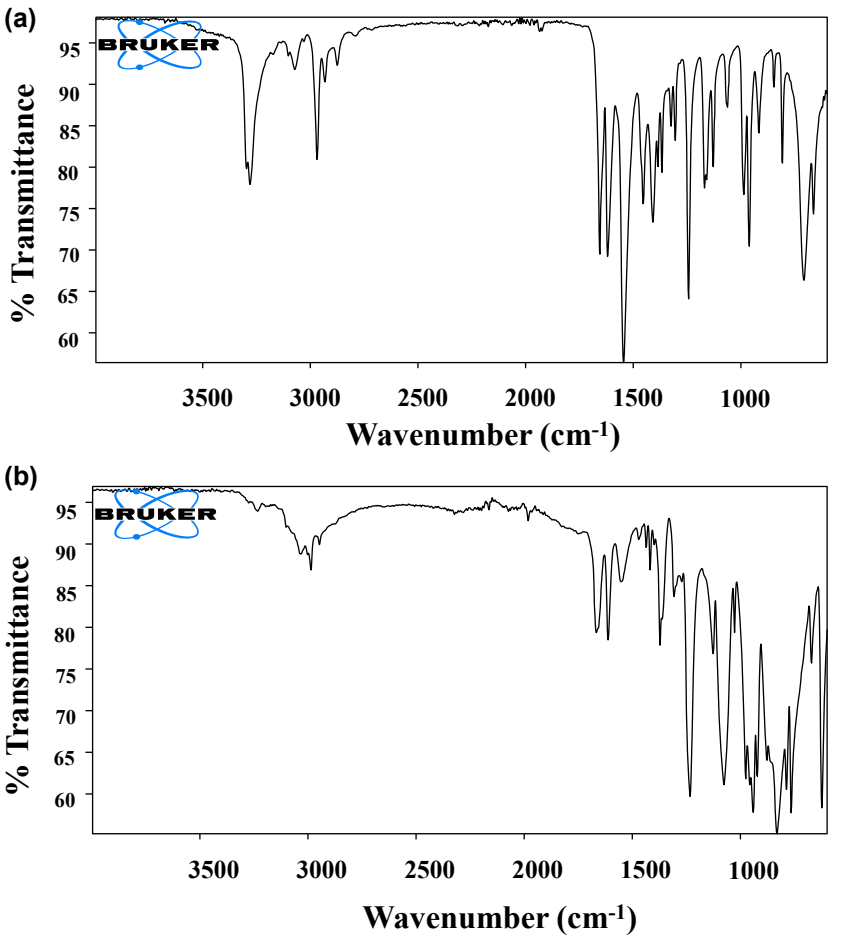

Figure 2: FTIR spectrum of initial monomers (a) NIPAM and (b) AMPS.

HG remain in the globule form due to dominance of polymer-polymer interaction. However, in the presence of water the hydrophilic groups interact with water molecules via hydrogen bonding and transformed into starched state resulting in the swelling of the hydrogel network. The water absorption capacity of HG was analyzed by adding small pieces of hydrogel in distilled water and allowing the hydrogel to absorb water at ambient conditions. The swelling was measured in terms of mass of the water absorbed by hydrogel. The swelling capacity has been represented in terms of swelling ratio versus time in Figure 4. The hydrogel absorbed distilled water 63 times of its weight in dried form. The swelling can also be observed from

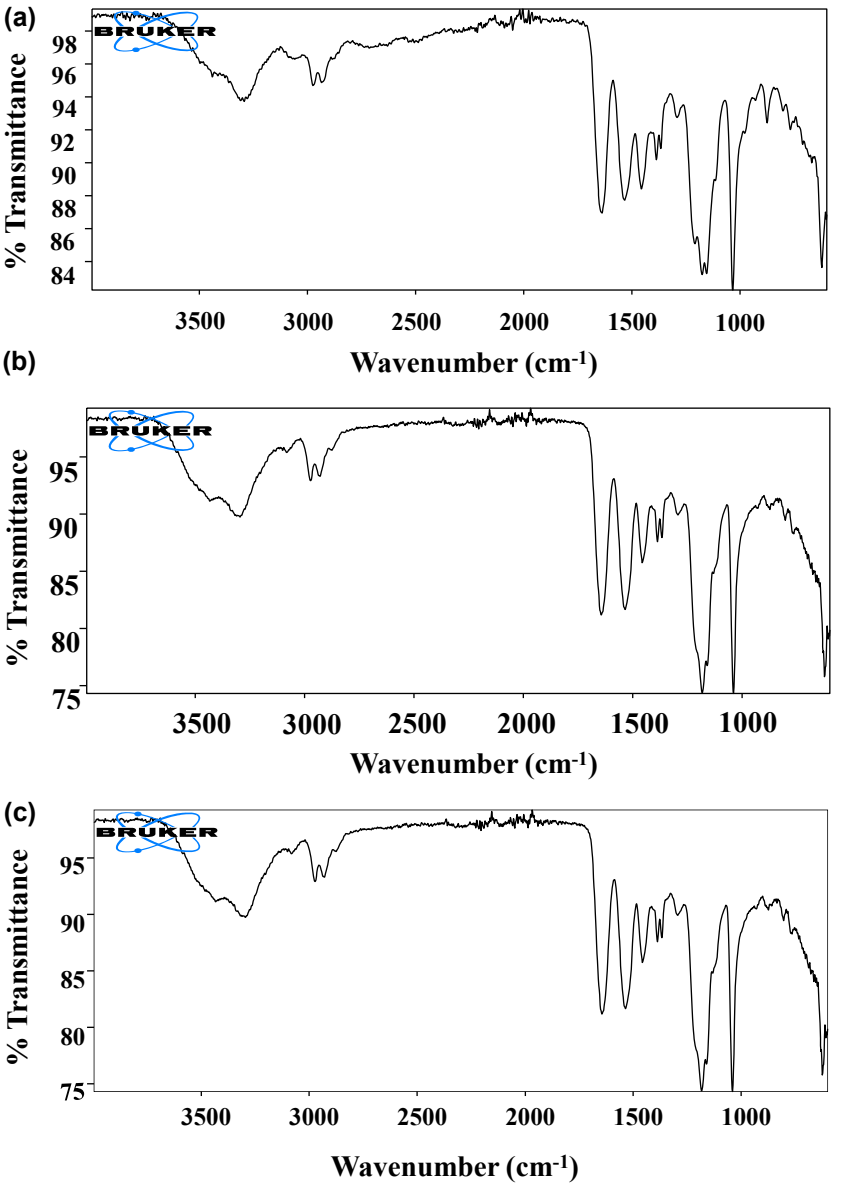

Figure 3: FTIR spectrum of (a) HG (b) Ni nanoparticles containing HG (c) Cu nanoparticles containing HG.

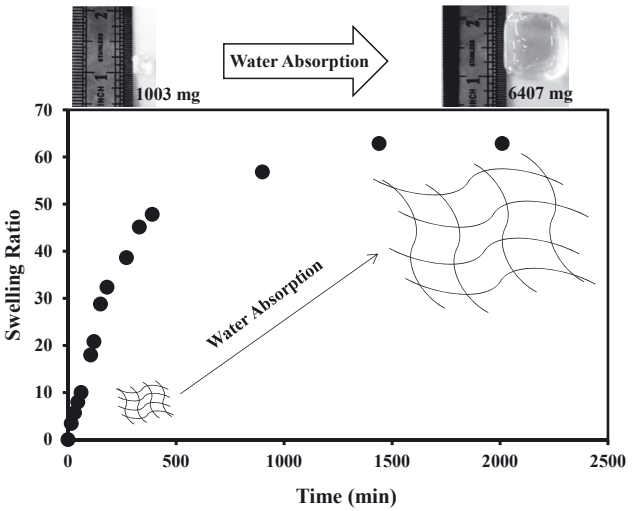

Figure 4: The physical appearance of dried and swollen HG and plot of swelling ratio as a function of time.

photographs (a) and (b) of hydrogel in the dried and swollen form, respectively, in Figure 4.

TEM was used to study the morphology of Ni and Cu nanoparticles and their dispersion in HG. Figure 5(a) and (b) demonstrate the TEM images of Ni and Cu nanoparticles loaded in HG. These TEM images indicate that the Ni and Cu nanoparticles were almost spherical in shape and well dispersed without any aggregation in the network of hydrogel. This dispersion of metal nanoparticles also represents that HG has not only served as reactor medium but also acted as an effective stabilizing agent for Ni and Cu nanoparticles once they were formed in the HG network. The average diameter of Ni and Cu nanoparticles loaded in the hydrogel are around 12.5 and 58 nm, respectively. The presence of Ni and Cu nanoparticles within HG were ensured from EDX spectroscopic analysis.

The spectrum of HG represents that sample material contains elements such as C, O, S, and N as shown in Figure 6(a). The EDX spectra of the Ni and Cu nanoparticles containing HG are represented in Figure 6(b) and (c). The spectra represent that sample material contains elements of hydrogel network as well as a significant amount of Ni and Cu. The weight percent of Ni and Cu is 14.5% and 10.7% respectively.

The HG and its corresponding composites with Ni and Cu nanoparticles were also subjected to XRD analysis to an idea about the amorphousity and crystallinity of the prepared sample. Figure 7 represents the XRD configuration of p(NIPAM-co-AMPS) hydrogel and its corresponding composites with both Ni and Cu nanoparticles.

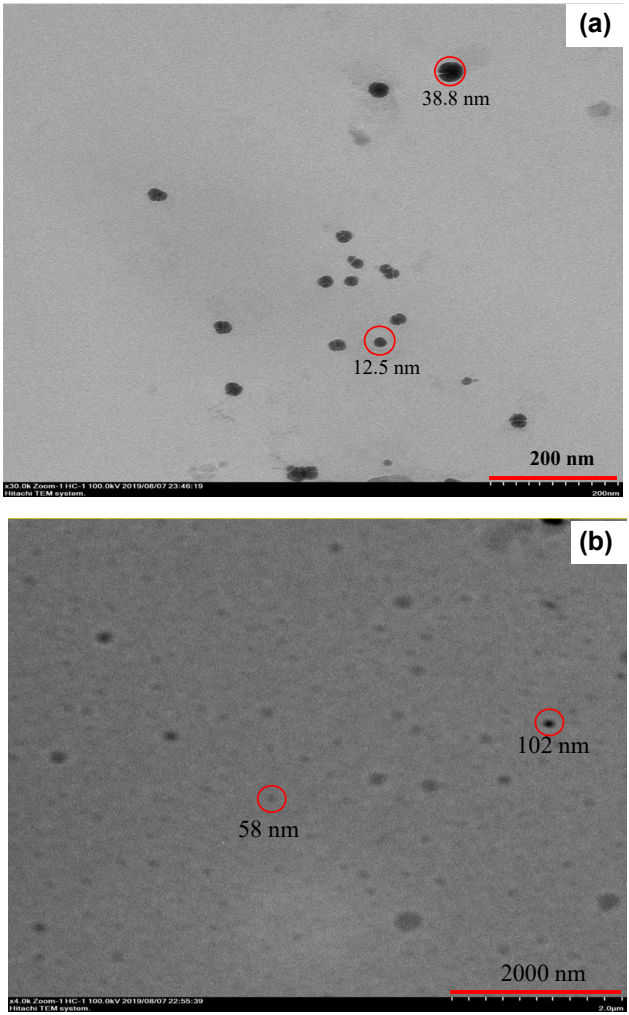

Figure 5: TEM image of (a) Ni and (b) Cu nanoparticles loaded in HG.

The bare hydrogel exhibited a broad diffraction peak around 2Θ value of 20 degree which matches to amorphous characteristic of the polymeric hydrogel [47]. The XRD pattern of Ni composite hydrogel depicts peaks around 2Θ values of 20, 30, 43, and 52 degrees which agree with the previous reports for Ni nanoparticles [48, 49]. In XRD pattern of Cu nanoparticles loaded hydrogel, two distinct peaks appear at around 2Θ value of 32 and 42 degree which correspond to CuO and Cu nanoparticles [50, 51]. The CuO can be formed due to oxidation of some Cu nanoparticles present at

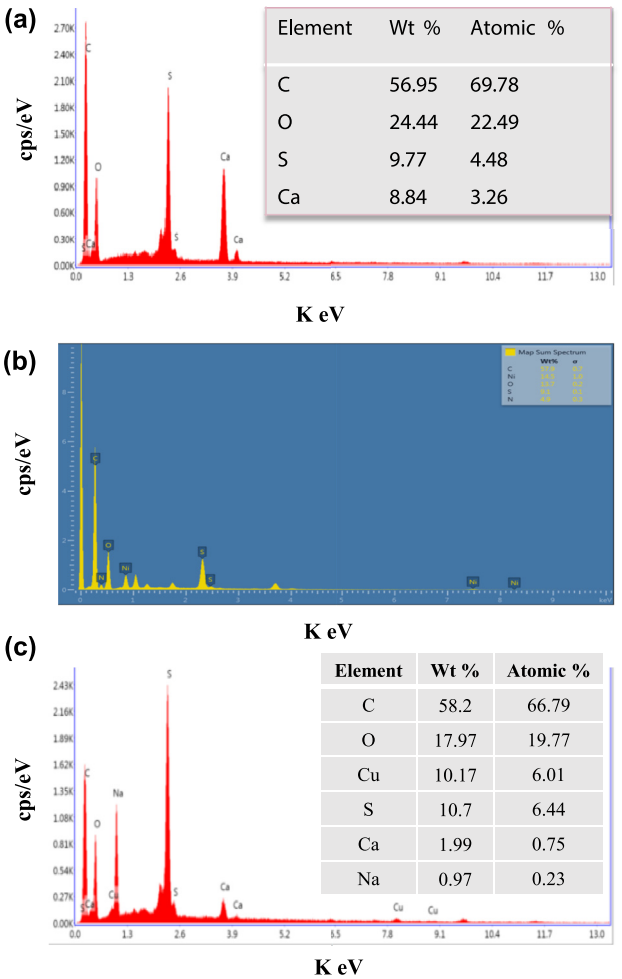

Figure 6: EDX spectrum of (a) HG (b) Ni nanoparticles containing HG (c) Cu nanoparticles containing HG.

the outer surface of hydrogel upon their exposure to air. Although Ni and Cu nanoparticles have crystalline configuration and therefore exhibit sharp peaks in XRD spectrum but when these nanoparticles are dispersed as discontinuous medium in an amorphous continuous medium, then synergistic effects of both the continuous and discontinuous mediums result in the broadness of peaks associated to Ni nanoparticles up to some extent as can be observed from Figure 7.

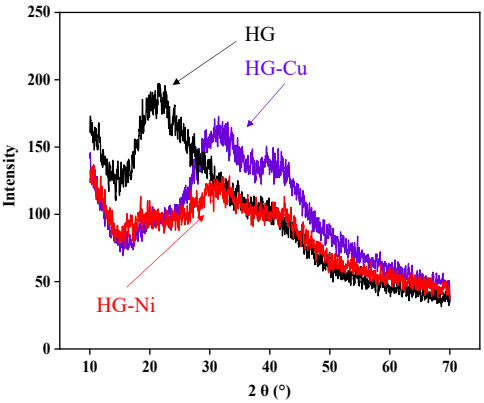

Figure 7: XRD pattern of HG, Ni nanoparticles containing HG, and Cu nanoparticles containing HG.

For thermal stability analysis the thermogram of HG in the temperature range of 50–750 °C were recorded and presented in Figure 8(a). The thermogram showed that bare HG has three distinct degradation temperature ranges of 50–140 °C, 240–335 °C, 335–500 °C with 9.4%, 43.4%, and 35.9% weight loss, respectively. The 1st weight loss can be associated with loss of water from hydrogel network. The 2nd weight loss is due to breakage of weakly cross-linked chains of hydrogel at external surface, while the 3rd weight loss can be related to thermal break down of internal cross-linked chains (where cross-linking density is high). The total weight loss of bare hydrogel in the temperature range 50–500 °C was 88.7%. The thermograms of HG containing Ni and Cu nanoparticles are given in Figure 8(b) and (c), respectively which show the higher thermal stability and over all lower weight loss ~65%. The higher thermal stability can be achieved due to the existence of metallic nanoparticles and their possible interaction with polymeric network while the overall lower weight loss is associated to the presence of metal contents which cannot be degraded below 750 °C. In the three-step thermal breakdown of the metal nanoparticles containing HG, the first step in the temperature range of 40–200 °C was associated to water loss. The second and third steps indicate weight loss due to lower cross-linked and higher cross-linked polymeric networks, respectively. The thermal degradation of metal nanoparticles containing HG was started around 340 °C. The initiation of thermal breakdown of HG containing metal nanoparticles at a temperature higher than that corresponding to the HG was obvious to the higher mechanical strength resulting from the possible interaction of metal nanoparticles with polymeric network. Irrespective of the mechanism of thermal breakdown, this analysis showed that these systems can be applied as catalysts below the reaction temperature of 340 °C.

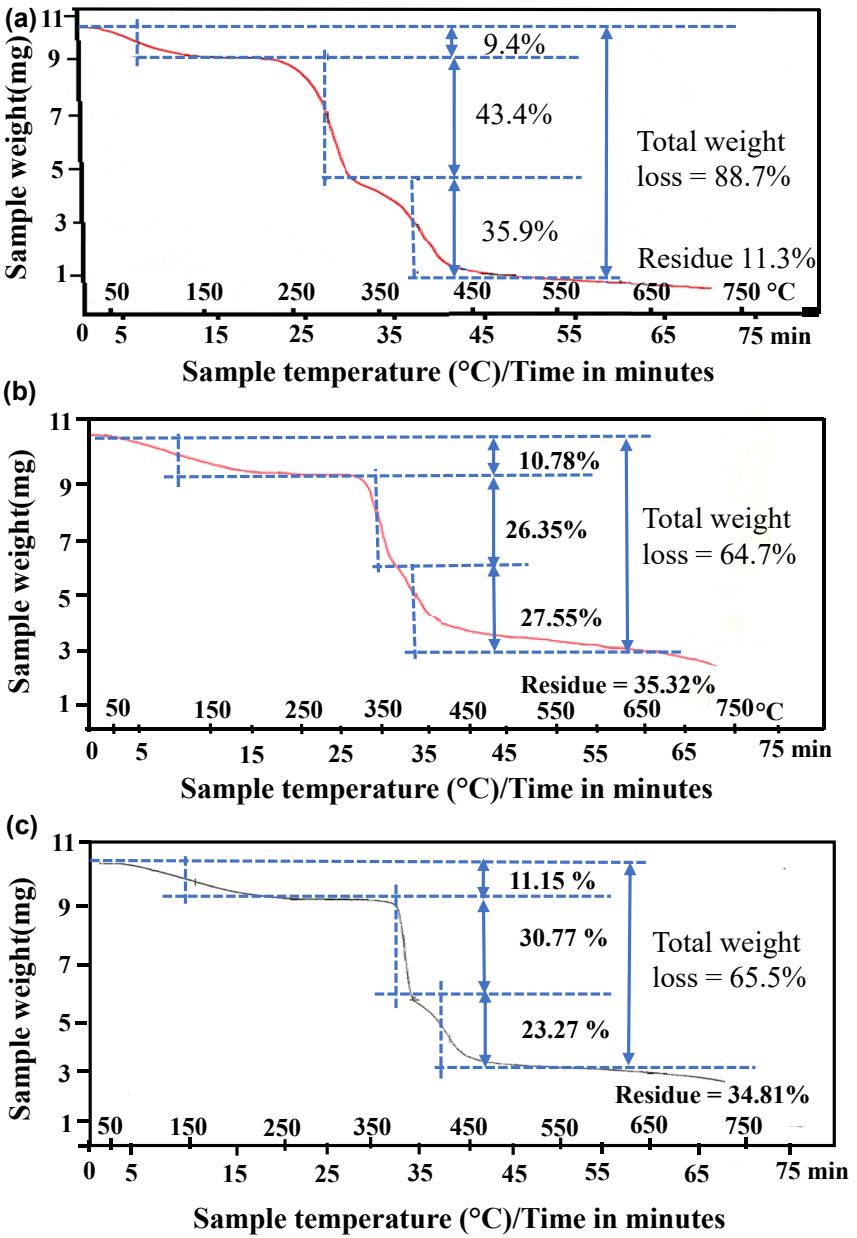

Figure 8: TGA thermogram of (a) HG (b) Ni nanoparticles containing HG (c) Cu nanoparticles containing HG.

3.2 Catalytic activity

4-NP is considered is considered as a toxic pollutant when contaminated in water from the various industries. To overcome the toxicity, 4-NP can be converted into 4-AP and the process requires the aid of a catalyst. Therefore, we have chosen this as model a reaction to test the catalytic activity of Ni and Cu metal nanoparticles containing HG. The reaction can be supervised with UV-Vis spectrophotometer by recording absorption of 4-NP and 4-AP at their maximum absorption wavelengths. A broad peak with maximum absorbance at 317 nm as shown in Figure 9(a) represents

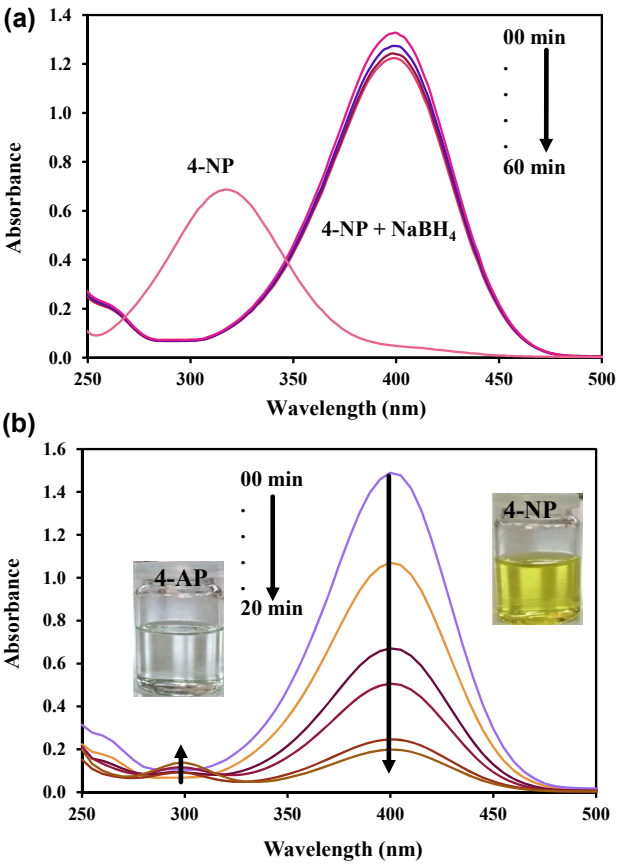

Figure 9: UV-Vis spectra for (a) the as-prepared aqueous solution of 4-NP, and 4-NP + $NABH_4$ as function of time (b) the reduction of 4-NP to 4-AP in the presence of Ni nanoparticles containing HG as a catalyst.

the presence of 4-NP in the aqueous solution. When reducing agent $NaBH_4$ was added in the aqueous solution of 4-NP, the maximum absorption peak was moved to 400 nm as shown in Figure 9(a). This change in absorption peak was observed because of conversion of 4-NP into phenolate ion upon its reaction with $NaBH_4$. As shown in Figure 9(a), only a meager amount of this 4-NP was changed into 4-AP when no catalyst was present in the reaction mixture. This is obvious because of large kinetic barrier between electron donor and acceptor of this reaction [52]. The presence of a suitable catalyst assists to overcome this energy barrier and ensures the proceeding of reaction at room temperature [53, 54]. When Ni or Cu metal nanoparticles containing HG was used as catalyst a remarkable increase in the reduction rate was observed and the reaction was almost completed in 20 min at 25 °C as evident from drop off absorbance of 4-NP at 400 nm. The emergence of new absorbance peak around 300 nm matches up with 4-AP which is the product of the subject reaction. Color of the reaction mixture changed progressively from yellow to transparent as shown by corresponding images in Figure 9(b) which also evidenced the reduction of 4-NP. It is noteworthy that the absorbance of 4-AP at 300 nm was much lower than that of 4-NP at 400 nm. It is due the difference in the values of molar absorptivity coefficient of 4-NP and 4-AP which is much higher for 4-NP. Therefore, although concentration of 4-AP was increased in reaction medium but only a little increase in its absorbance was observed due to very low value of its molar absorptivity coefficient. It has been reported in literature that the rate of this reaction depends on the amount of reducing agent, but the rate becomes independent on the amount of reducing agent when it is used in 100 times surplus with reference to 4-NP.

In this study, reducing agent was used 100 times more with reference to 4-NP and the reaction was thought to follow the pseudo first order kinetics. Therefore, rate of reaction was computed by using this kinetic model. The application of pseudo first order kinetics for the calculation of rate of reaction, which is apparent rate of reaction (k_{app}) in real sense, is shown in Figure 10(a). The value of apparent rate constant (k_{app}) was computed as 0.1041 and 0.1225 min^{-1} for the reduction of 4-NP catalyzed by HG containing Ni and Cu nanoparticles, respectively.

The catalytic activity of Ni nanoparticles containing HG was also observed at 48, 65, 76 and 88 °C. As expected with the rise in temperature, the rate of reaction was also enhanced. The rise in rate of reaction with rise in temperature can be reasoned in a way that average kinetic energy of molecules is enhanced which subsequently enhances the rate of diffusion of reactant molecules into hydrogel containing metal nanoparticles as well as collusion frequency of reactants and catalyst. This enhancement of diffusion rate and collusion number further enhance the rate of adsorption of reactants on the surface of catalysts and hence the conversion of reactants into products. However, relatively small increase in the reduction rate was observed in the temperature range of 48–65 °C as in Figure 10(b). This can be

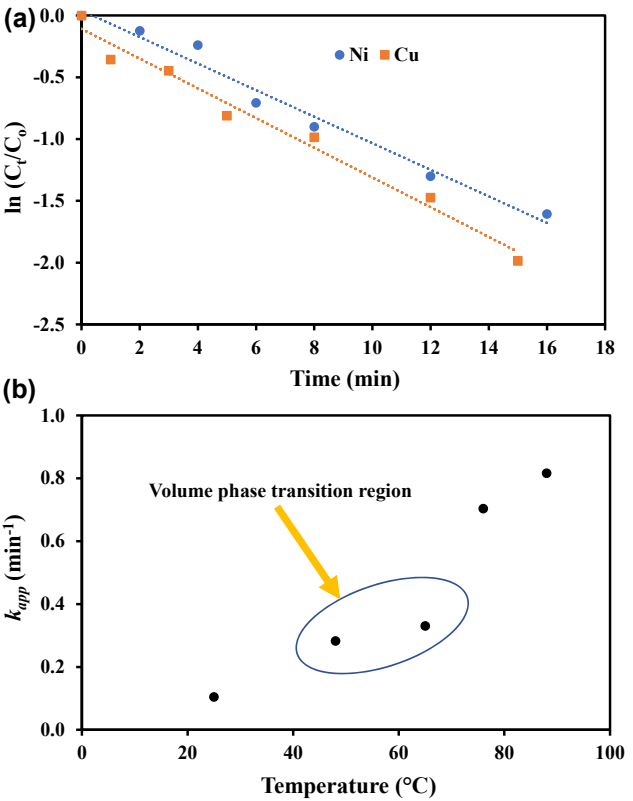

Figure 10: Plots of pseudo first order kinetics for the reduction of 4-NP catalyzed by Cu and Ni nanoparticles containing HG at 25 °C (a) plot for k_{app} at different temperatures for the reduction of 4-NP catalyzed by Ni nanoparticles containing HG (b).

observed due to shrinking of hydrogel network in this temperature window. The HG contains NIPAM which is temperature responsive substance and shrinks at 32 °C. When NIPAM is copolymerized with hydrophilic substance such as AMPS, then the volume phase transition is shifted to higher temperature. When hydrogel network shrinks, the polymer chains come close to each other. As a result, resistance of the polymer network against the diffusion of reactants into the hydrogel network increases slightly. Therefore, meager boost in rate of reaction was recorded in this temperature window. The further enhancement in temperature displayed a larger rise in rate of reaction showing that there was no more shrinking in hydrogel network. The k_{app} was increased from 0.1041 to 0.8156 m^{-1} with corresponding increase of temperature from 25 to 88 °C. These results demonstrate that catalytic activity of the prepared catalyst was not damaged by increasing the temperature.

3.3 Reusability of catalyst

Recovery of the catalyst from the reaction medium and its recycling is an important feature of a catalyst for real applications. Keeping in view this important aspect, the catalyst was recycled by separating from the reaction medium via filtration through a special filter paper known as plankton cloth filter at the end of the reaction. The filtered catalyst was then washed with plenty of water to ensure the desorption of all species which were adsorbed on it during previous cycle. The washed catalyst was transferred in the reaction medium for the next cycle and the reaction was observed under same reaction conditions. The change in activity was measured in terms of change in rate of reaction in every successive cycle. In case of Cu nanoparticles containing HG catalytic activity was increased in second cycle as shown in Figure 11(a). This increase in the activity may be due to the removal of impurities from active sites during washing after first cycle.

In the third cycle, the catalytic activity was decreased to 68% which was almost remained constant till fifth cycle however, almost 100% of the reactants were converted into the product in every cycle. The decline in catalytic activity may be associated to the formation of metal oxide layer (because Cu nanoparticles can oxidize readily) on the surface of catalyst leading to a loss in active sites. Another reason might be some loss of catalyst during the process of recycling. Surprisingly, Ni nanoparticles containing HG was observed to be dissolved gradually in the recycling process as shown in Figure 11(b). Therefore, a 65% loss in the catalytic activity was observed in the third cycle. This can be observed to weaker interaction of Ni with functional groups of polymeric networks. In addition to the structural breakdown and loss of catalytic sites in every cycle, the oxidation Ni nanoparticles may also contribute to the loss of its catalytic activity. So, the recycling study revealed that HG containing Cu nanoparticles was more advantageous catalyst than that containing Ni nanoparticles.

4 Conclusions

A hydrogel was successfully synthesized by simultaneous cross-linking and copolymerization of NIPAM and AMPS via free radical polymerization at ambient conditions. The FTIR results identified the polymerization reaction and existence of corresponding functional groups. The prepared HG showed hydrophilic character by absorbing water 63 times of its weight in dried form. The prepared hydrogel was applied as reactor for synthesizing Ni and Cu Nanoparticles. From TEM analysis it was found that both Ni and Cu nanoparticles were almost spherical in shape and

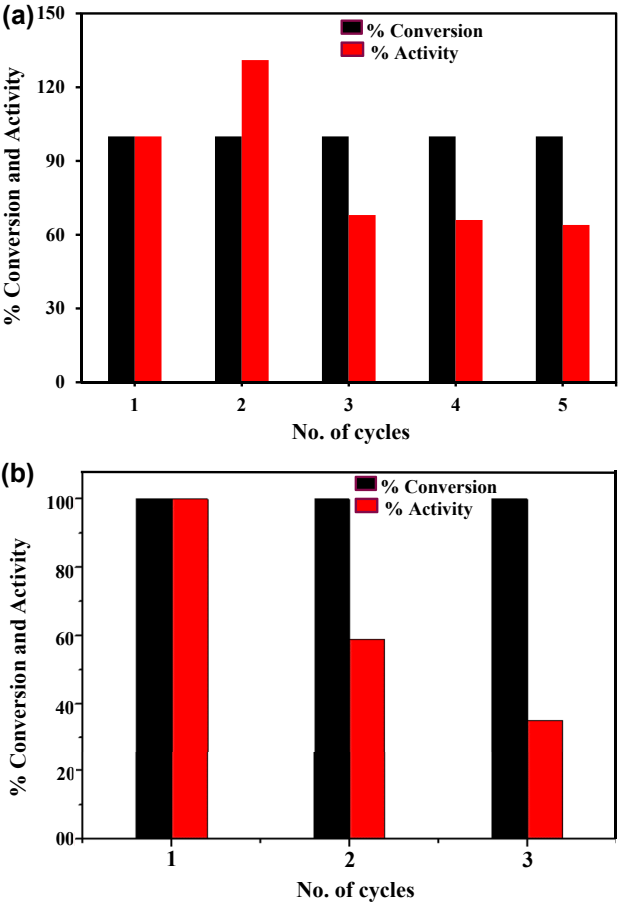

Figure 11: Recycling results of (a) Cu and (b) Ni nanoparticles containing HG in the reduction of 4-NP in terms of % activity of catalyst and % conversion of reactants in every cycle.

well dispersed. The diameters of the Ni and Cu nanoparticles were mostly found around 12.5 and 58 nm, respectively. The formation of homogenous shaped and well dispersed nanoparticles of both the metals showed that HG has acted as a reactor as well as an effective stabilizing agent. The as-prepared Ni and Cu nanoparticles containing HG were found efficient catalysts for the reduction of 4-NP. At 25 °C, the reduction of 4-NP was found to proceed with apparent rate constant (k_{app}) of 0.107 and 0.122 min^{-1} in the presence of composite containing Ni and Cu nanoparticles, respectively. However, k_{app} was increased with corresponding increase in temperature and its maximum value was found to be 0.815 min^{-1} at 88 °C with catalyst

containing Ni nanoparticles. Although catalytic activity of both the catalysts was observed almost equivalent but Cu nanoparticles containing catalyst was found to better recycling ability.

Author contributions: All the authors have accepted responsibility for the entire content of this submitted manuscript and approved submission.
Research funding: None declared.
Conflict of interest statement: The authors declare no conflicts of interest regarding this article.

References

1. Liu D. X., Mu J., Yao Q., Bai Y., Qian F., Liang F., Shi F. N., Gao J. *SN Appl. Sci.* 2019, *1*, 184.
2. Dong Z., Le X., Dong C., Zhang W., Li X., Ma J. *Appl. Catal, B* 2015, *162*, 372.
3. Vellaichamy B., Prakash P., Thomas J. *Ultrason. Sonochem.* 2018, *48*, 362.
4. Rashed M. N., Ed. *Organic pollutants-monitoring, risk and treatment*; BoD–Books on Demand, 2013; p. 167.
5. Tijani J. O., Fatoba O. O., Madzivire G., Petrik L. F. *Water Air Soil Pollut.* 2014, *225*, 1.
6. Santi C., Cortes S., D'Acqui L., Sparvoli E., Pushparaj B. *Bioresour. Technol.* 2008, *99*, 1945.
7. Ye S., Chen Y., Yao X., Zhang J. *Chemosphere* 2021, *273*, 128503.
8. Ma M., Yang Y., Li W., Feng R., Li Z., Lyu P., Ma Y. *J. Mater. Sci.* 2019, *54*, 323.
9. Yan Z., Fu L., Zuo X., Yang H. *Appl. Catal, B* 2018, *226*, 23.
10. Ajmal M., Siddiq M., Al-Lohedan H., Sahiner N. *RSC Adv.* 2014, *4*, 59562.
11. Revathy T., Dhanapal K., Dhanavel S., Narayanan V., Stephen A. *J. Alloys Compd.* 2018, *735*, 1703.
12. Mitsudome T., Mikami Y., Funai H., Mizugaki T., Jitsukawa K., Kaneda K. *Angew. Chem. Int. Ed.* 2008, *47*, 138.
13. Waszczuk P., Barnard T. M., Rice C., Masel R. I., Wieckowski A. *Electrochem. Commun.* 2002, *4*, 599.
14. Lang H., Maldonado S., Stevenson K. J., Chandler B. D. *J. Am. Chem. Soc.* 2004, *126*, 12949.
15. Zhu J., Zhang X., Qin Z., Zhang L., Ye Y., Cao M., Gao L., Jiao T. *Colloids Surf. A Physicochem. Eng. Asp.* 2021, *611*, 125889.
16. Deraedt C., Ye R., Ralston W. T., Toste F. D., Somorjai G. A. *J. Am. Chem. Soc.* 2017, *139*, 18084.
17. Barman S. R., Nain A., Jain S., Punjabi N., Mukherji S., Satija J. *J. Mater. Chem. B* 2018, *6*, 2368.
18. Yang Q., Li L., Zhao F., Wang Y., Ye Z., Hua C., Liu Z., Bohinc K., Guo X. *Nanomaterials* 2020, *10*, 799.
19. Pocoví-Martínez S., Cassano D., Voliani V. *ACS Appl. Nano Mater.* 2018, *1*, 1836.
20. Gao Z., Zhang Y., Li D., Werth C. J., Zhang Y., Zhou X. *J. Hazard Mater.* 2015, *286*, 425.
21. Xu P., Cen C., Chen N., Lin H., Wang Q., Xu N., Tang J., Teng Z. *J. Colloid Interface Sci.* 2018, *526*, 194.
22. Robinson D. A., Liu Y., Edwards M. A., Vitti N. J., Oja S. M., Zhang B., White H. S. *J. Am. Chem. Soc.* 2017, *139*, 16923.
23. Clasky A. J., Watchorn J. D., Chen P. Z., Gu F. X. *Acta Biomater.* 2021, *122*, 1.

24. Wu X. Q., Wu X. W., Huang Q., Shen J. S., Zhang H. W. *Appl. Surf. Sci.* 2015, *331*, 210.
25. Pandey N., Shukla S., Singh N. *Nanocomposites* 2017, *3*, 47.
26. Thakur S., Verma A., Sharma B., Chaudhary J., Tamulevicius S., Thakur V. K. *Curr. Opin. Green Sustain. Chem.* 2018, *13*, 32.
27. Zohuriaan-Mehr M. J., Kabiri K. *Iran. Polym. J.* 2008, *17*, 451.
28. Tran VV., Park D., Lee Y. C. *Environ. Sci. Pollut. Res.* 2018, *25*, 24569.
29. Qi X., Lin L., Shen L., Li Z., Qin T., Qian Y., Wu X., Wei X., Gong Q., Shen J. *ACS Sustain. Chem. Eng.* 2019, *7*, 11014.
30. Chung B. G., Lee K. H., Khademhosseini A., Lee S. H. *Lab Chip* 2012, *12*, 45.
31. Narayanaswamy R., Torchilin V. P. *Molecules* 2019, *24*, 603.
32. El-Hoshoudy A., Mohammedy M., Ramzi M., Desouky S., Attia A. *J. Mol. Liq.* 2019, *277*, 142.
33. Chen L., Zhu X., Fu M., Zhao H., Li G., Zuo J. *Colloids Surf. A Physicochem. Eng. Asp.* 2019, *570*, 251.
34. Dong C. M., Liu G. *Polym. Chem.* 2013, *4*, 46.
35. Shah R. A., Frazar E. M., Hilt J. Z. *Curr. Opin. Chem. Eng.* 2020, *30*, 103.
36. Chevry M., Menuel S., Leger B., Noel S., Monflier E., Hapiot F. *New J. Chem.* 2019, *43*, 9865.
37. Niu Y., Guo T., Yuan X., Zhao Y., Ren L. *Soft Matter* 2018, *14*, 1227.
38. Niu Y., Yuan X., Zhao Y., Zhang W., Ren L. *Macromol. Chem. Phys.* 2017, *218*, 1600540.
39. Rajabi M., McConnell M., Cabral J., Ali M. A. *Carbohydr. Polym.* 2021, *260*, 117768.
40. Veiga A. S., Schneider J. P. *Peptide Sci.* 2013, *100*, 637.
41. Kureha T., Nagase Y., Suzuki D. *ACS Omega* 2018, *3*, 6158.
42. Cyganowski P., Jermakowicz-Bartkowiak D., Jamroz P., Pohl P., Dzimitrowicz A. *Colloids Surf. A Physicochem. Eng. Asp.* 2019, *582*, 123886.
43. Li X., Dong F., Zhang L., Xu Q., Zhu X., Liang S., Hu L., Xie H. *Chem. Eng. J.* 2019, *372*, 516.
44. Feng Y., Yin J., Liu S., Wang Y., Li B., Jiao T. *ACS Omega* 2020, *5*, 3725.
45. Berillo D., Cundy A. *Carbohydr. Polym.* 2018, *192*, 166.
46. Bogireddy N. K. R., Sahare P., Pal U., Méndez S. F. O., Gomez L. M., Agarwal V. *Chem. Eng. J.* 2020, *388*, 124237.
47. Haleem A., Chen J., Guo X. X., Wang J. Y., Li H. J., Li P. Y., Chen S. Q., He W. D. *Polymer* 2020, *193*, 122352.
48. Zhao L., Li Q., Su Y., Yue Q., Gao B. *Int. J. Hydrogen Energy* 2017, *42*, 6746.
49. Pandey A., Manivannan R. *Recent Pat. Nanomed.* 2015, *5*, 33.
50. Pinedo-Guerrero Z. H., Hernández-Fuentes A. D., Ortega-Ortiz H., Benavides-Mendoza A., Cadenas-Pliego G. *Molecules* 2017, *22*, 926.
51. Abdollahi Z., Zare E. N., Salimi F., Goudarzi I., Tay F. R., Makvandi P. *Int. J. Mol. Sci.* 2021, *22*, 2531.
52. Zhang J., Yan Z., Fu L., Zhang Y., Yang H., Ouyang J., Chen D. *Appl. Clay Sci.* 2018, *166*, 166.
53. Pandey S., Mishra S. B. *Carbohydr. Polym.* 2014, *113*, 525.
54. Hashimi A. S., Nohan M. A. N. M., Chin S. X., Zakaria S., Chia C. H. *Nanomaterials* 2019, *9*, 936.